REMOTE MONITORING OF ENERGY-AUTONOMOUS CONSTRUCTED WETLANDS

Simão P.B. Lopes[1], Manuel F.M. Barros[1], Carlos A.F. Ferreira[1], Dina M.R. Mateus[2], Pedro M.G. Matos[1], Pedro M.S. Neves[3], Henrique J.O. Pinho[1*]

[1]Ci2, Smart Cities Research Center, Instituto Politécnico de Tomar, Estrada da Serra, 2300-313 Tomar, Portugal

[2]Techn&art, Centre for Technology, Restoration and Art Enhancement, Instituto Politécnico de Tomar, Estrada da Serra, 2300-313 Tomar, Portugal

[3]Lab.IPT, Instituto Politécnico de Tomar, Estrada da Serra, 2300-313 Tomar, Portugal

Abstract

Constructed Wetlands systems (CW) are nature-based and sustainable technology for treating wastewater, contributing to the management and protection of freshwater resources. Moreover, CW can contribute to valorizing waste materials, producing reclaimed water for diverse applications, and producing plant biomass that can be material and energetically valorized. Because CW efficiency depends on several mechanisms such as physical, chemical, and biological, its real-time monitoring is essential to provide a better use of this technology. This work describes a smart framework for monitoring CW based on IoT devices and sensors, and data science tools providing real-time processing of gathered water quality parameters and environmental variables. Furthermore, the framework manages renewable energy sources to provide the required energy for CW operation and monitoring. Data collected from the sensor network show significant daily variations in water quality parameters. The future processing of these data can provide the development of models to improve the efficiency of the CW.

Keywords: *constructed wetlands, water quality monitoring, real-time analysis, embedded systems, distributed control systems, photovoltaic systems*

1. INTRODUCTION

Efficient and sustainable processes for wastewater treatment and reuse are mandatory for the protection of water resources [1-4]. Affordable means for wastewater treatment can avoid threats to freshwater availability for basic human needs, crops, and feed production, can avoid diseases and negative environmental impacts, and can potentiate the reuse of the treated wastewater [5-6]. Reclaimed water, as usually the recovered treated wastewater is named, can be used for diverse applications, such as irrigation, washing, fire control, and process water in the industry [7-12]. All applications of reclaimed water contribute to diminishing the abstraction of water from nature.

Wastewater can be treated by several conventional technologies, including physical, chemical, and biological processes [2,12]. Due to the need for sustainable and low-impact technologies, nature-based solutions (NBS) are being considered as an alternative to conventional technologies [13,14]. Among NBS, CW is an affordable and greener technology for wastewater treatment [10,11].

The main components of CW are an impermeabilized basin or lagoon and aquatic plants (macrophytes). In free surface flow CW the macrophytes are of floating species (Fig. 1a), or rooted species fixed on a supporting matrix (Fig. 1b). In subsurface flow CW, the macrophytes are rooted in the supporting matrix (Fig. 1c).

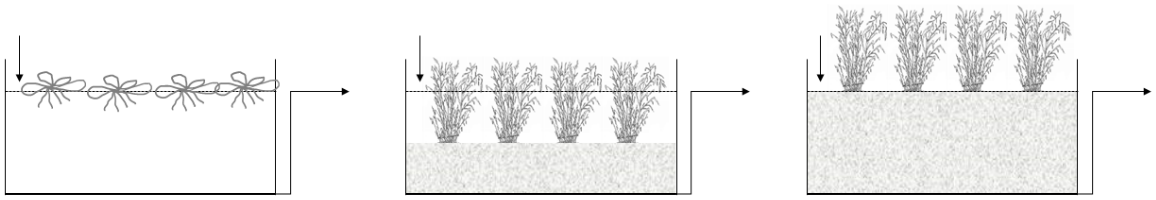

Fig. 1. Typical schemes of CW main types: (a,b) Free surface flow CW; (c) Subsurface flow CW.

Besides supporting the macrophytes, the CW matrix can directly contribute to the wastewater treatment, or indirectly via the availability of surface area to the development of biofilms [15,16].

CW are designed to mimic natural wetlands to efficiently treat wastewater through a combination of mechanisms [17,18]: (i) filtration, sedimentation, adsorption, and precipitation, among other physical and chemical phenomena promoted by the CW matrix; (ii) assimilation of nutrients by the macrophytes; (iii) breakdown and assimilation of biodegradable water pollutants by microorganisms. Because these mechanisms are all complex and interconnected, and depending on the environment, such as air temperature and humidity, rainfall, wind speed, and solar radiation, the optimization of CW operation depends on the simultaneous knowledge of several variables [17,18].

In addition to the environmental parameters referred to above, several water quality parameters should be evaluated, depending on the type of wastewater and the application of the treated water (Portuguese Decree-Law. No. 119 of 2019; EU Regulation 2020/74 of the European Parliament and the Council of 25 May 2020 on minimum requirements for water reuse). Usual water quality parameters include physical parameters, such as suspended solids, electrical conductivity, and temperature, chemical parameters, such as such as pH, nutrients (nitrogen and phosphorous compounds), and chemical oxygen demand, and biological parameters, such as biochemical oxygen demand, and pathogenic microorganisms [10,18].

CW monitoring, like the monitoring of conventional wastewater treatment technologies, is typically made by the evaluation of the water quality parameters in chemical laboratories, after samples collection on site. This is a costly and time-consuming procedure and implies a delay on results availability. The current development of IoT resources and the increasing availability of electrochemical sensors allows to the implementation of sensors-based networks [19]. Electrochemical sensor networks can provide real-time access to water quality parameters, depending on the availability of sensors for the relevant parameters.

This work describes the development of a sensor network for real-time data acquisition and processing of a set of water quality parameters, in the input and output stream of a pilot-scale CW. The acquired data allow the continuous evaluation of the CW’s treatment efficiency, granting a better knowledge of the complex mechanisms underlying the wastewater treatment.

Furthermore, considering that CW can be a solution for decentralized wastewater treatment plants, a photovoltaic system supported by batteries is proposed to guarantee the power requirements for the CW and sensor network.

2. FRAMEWORK FOR REMOTE MONITORING OF CW

Figure 2 illustrates the main scheme of the implemented remote monitored and energy-autonomous CW system pilot-plant.

The wastewater is initially maintained in a storage tank, and from there, it is pumped into a downstream container where water analysis takes place. The water then flows by gravity to a tank filled with a mixture of recovered solid waste fragments supporting macrophyte plants (common reed, *Phragmites australis*). Again, aided by gravity and the siphon effect, the output treated water falls into another container where further analysis is conducted. When the water level reaches a certain threshold, a low-flow pump is activated to transport the treated water to another tank for storage.

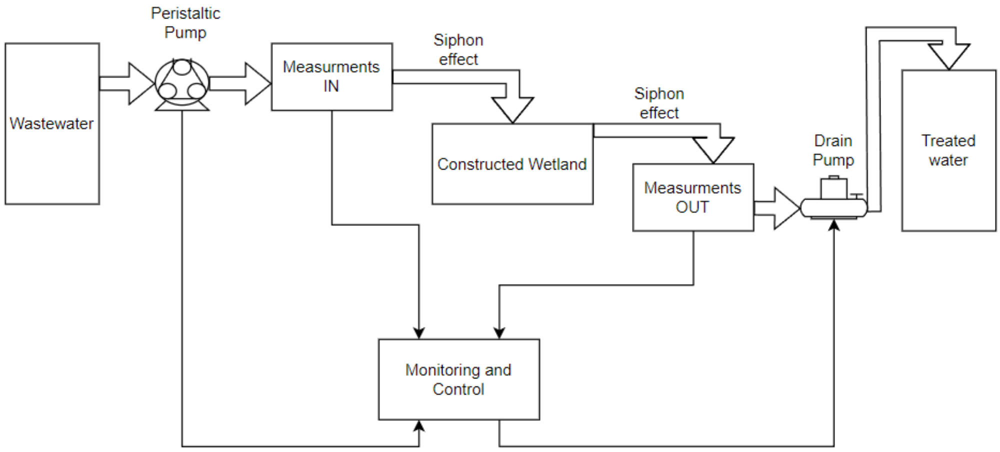

Fig. 2. Block Diagram of the remote monitoring CW system.

A Distributed Control System (DCS) is responsible for the monitoring, control, and actuation of the sensor network, pumps, and the renewable energy system. This DCS relies greatly on microcontrollers, microprocessors, sensors, and actuators. Sensors gather critical incoming information from the process, at the same time microcontrollers receive, process, and send the sensor data to an in-house developed cloud platform (MRIPTA). When the need arises, the microcontrollers operate the actuators.

In this section, we present a comprehensive outline of the materials used to construct the DCS for the chemical process. We will delve into the specific purpose of each material within the system and elaborate on the parameters they measure. The pivotal role of sensors will be discussed in detail, encompassing the crucial process variables they monitor. Furthermore, we will explore the various actuators employed and the specific control functions they execute to manipulate the process variables.

In addition to sensor and actuator discussions, we will provide insights into the microcontrollers and microprocessors that form the intelligent core of the DCS. These processing units receive and process data from the sensors, making informed decisions and generating control signals to actuate the system. The communication protocols utilized to facilitate seamless data transmission between different points within the DCS will also be examined, ensuring real-time monitoring and control of the CW.

Finally, we will introduce and clarify the low and high-level firmware routines integrated into the DCS. These routines play a crucial role in optimizing the control strategies and overall performance of the system. Understanding the functionality of these firmware routines will provide valuable insights into the adaptability and efficiency of the DCS in managing the complexities of the CW effectively.

2.1. Sensors

The treated water must comply with a series of parameters required by the regulations (such as the Portuguese Decree-Law no. 152/97, and the EU Directive no. 91/271/CEE). Although most of the required parameters are evaluated by standard analytical methods carried out in the laboratory after water sampling, some parameters can be evaluated by physical or electrochemical sensors. The use of sensors can allow almost real-time evaluation of those parameters, providing means to improve the monitoring and optimization of the wastewater treatment process.

The pilot plant includes a set of sensors to acquire data on several parameters of water quality, in the input and output streams as presented in Fig. 2: Temperature; pH; Electrical Conductivity (EC), for the evaluation of the overall presence of ions in the water; Turbidity, measuring the presence of suspended particles, in Nephelometric Turbidity Units (NTU); Light absorbance at 254 nm, which is an indicator of organic compounds. In addition to the parameters mentioned above, the concentration of phosphates, nitrates, among others ions, was determined through an integrated sensor system from Clean Grow (CG200).

Moreover, a compact weather station provides environmental data, such as wind speed, air temperature, humidity, rainfall, and solar radiation. The information provided by the weather station helps to determine the relevance of the measured parameters to the wastewater treatment process.

Finally, capacitive level sensors were utilized to measure the water level in the output measuring container. These sensors do not require direct contact with the liquid.

2.2. Actuators

To control the water flow at the inlet and outlet of the CW, two different pumps were used. The input pump can be actuated by a control loop, to regulate the water flow through the CW. Regulation of water flow could be a way to optimize the efficiency of the CW, responding to water loss to the atmosphere due to evaporation and evapotranspiration, and water gain by rainfall.

In the CW's output water stream, two-level sensors are employed to effectively control the water drainage flow. Two water level sensitive sensors were applied to activate and deactivate an output pump located in the output container, cycling and pumping the treated water into the water storage vessel.

2.3. Microcontroller and microprocessors

To establish communication between the various sensors and actuators two ESP32 microcontrollers were used. These microcontrollers have two cores, WiFi and Bluetooth connectivity. They operate at a voltage of 3.3 V and consume an average of 100 mA. The logic level voltage HIGH available on each General-Purpose Input/Output (GPIO) pin is 3.3 V, and they can provide a maximum current of 40 mA at their output terminals.

Each of the microcontrollers is responsible for collecting, aggregating, and forwarding information from all the sensors at the inlet and outlet to the microprocessor. It is also important to note that the ESP32 at the inlet is responsible for controlling the inlet flow with the help of the peristaltic pump, while the ESP32 at the outlet is responsible for measuring the flow at the system's outlet.

A Raspberry Pi (Rpi) with the Bullseye 11 operating system was used as an edge device between the process and the database. The Rpi is responsible for receiving sensor parameters sent by the microcontrollers and the Clean Grow module, combining all the data in JSON format, and sending them to the database.

2.4. Communication protocols

In order to establish effective data exchange between the sensors, actuators, and central processing units, the selection and configuration of these protocols are essential for maintaining reliable and secure communication within the system.

Furthermore, since the sensors used were not all from the same supplier, and there was a need to forward information to different devices, it was necessary to employ a series of communication protocols. In this project, five distinct communication protocols are being used. Short-range, medium-range, and long-range protocols are being employed. These are the following: I2C (Inter-Integrated Circuit); Modbus RTU (Remote Terminal Unit); UART (Universal Asynchronous Receiver-Transmitter); HTTP (Hypertext Transfer Protocol); and MQTT (Message Queuing Telemetry Transport).

The I2C is a low-range and low-level protocol commonly used for embedded system applications. It is a synchronous and half-duplex protocol, meaning it requires a clock frequency and it is bidirectional, but does not allow simultaneous data transmission. [20]. In the case of this work, the I2C protocol is being used to establish communication between the microcontrollers (ESP32) and the Atlas Scientific sensors.

The Modbus RTU protocol is a medium/long-range protocol primarily used in the industry. It operates at a high level and is based on the RS-485 physical standard, utilizing the master/slave communication principle. Up to 247 devices can be connected to the Modbus network, each with a unique ID. This protocol communicates over a two-wire (pair) connection, typically twisted together to minimize inductance and parasitic capacitance, which can cause crosstalk. The Modbus communication protocol is a half-duplex protocol and uses two bus lines commonly known as A and B [21].

The Modbus protocol is being used in conjunction with the transceiver MAX485 integrated circuit to establish communication between the peristaltic pump, turbidity sensor, and organic load sensor with the microcontrollers. With the help of this protocol it is possible to collect and send relevant information to the process, such as reading the speed of the peristaltic pump, retrieving parameter values from other sensors, or even changing some parameters.

The UART protocol is an asynchronous, low-level, and short-range protocol based on the RS-232 physical standard [22]. This protocol is employed to establish communication between only two devices, typically in embedded systems, which creates a significant disadvantage compared to protocols like I2C or SPI (Serial Peripheral Interface). UART operates by crossing the Rx and Tx pairs and connecting the ground between both devices. In this work, UART is used to bridge the Modbus protocol and the microcontrollers. With the help of the Max485 IC and a code library, data is transmitted and received via UART (RS-232).

The MQTT protocol is a high-level protocol based on the TCP/IP protocol [23]. This protocol operates on the principle of topic subscription and publishing, where messages are sent and received within these topics. Typically, this protocol relies on a broker, which is hosted on a computer or microprocessor. The MQTT broker acts as an intermediary, that receives all messages from the MQTT clients and then routes the messages to the appropriate subscribing clients. The broker functions as a postman [24].

MQTT is being used to send sensor readings from the microcontrollers to the microprocessor (Raspberry Pi). It is also the chosen protocol for establishing communication between the process and the database.

The HTTP protocol is a high-level protocol based on the application layer [25]. In this work, this protocol primarily functions using the PUT and GET methods. HTTP is being used to establish communication between the Rpi and the CleanGrow module. With this protocol, it is possible to read the values given by the sensor module, and send requests for new analysis, cleaning, or calibration.

In the DCS, these protocols serve as the backbone for data transmission and enable seamless communication between different devices and components. Overall, the selection and utilization of these communication protocols were crucial in establishing efficient and reliable communication channels within the system. Each protocol was chosen based on its specific characteristics and compatibility with the devices and components involved. By leveraging these protocols, the DCS achieved seamless data transmission, control, and integration, enabling effective monitoring and management of the industrial control and electronics processes.

2.5. Embedded systems firmware and algorithms

Embedded systems programming involves developing firmware specifically tailored for microcontrollers. These routines are tailored to meet the unique requirements and constraints of the ESP32, such as limited processing power, memory, and energy resources.

In order to create a robust set of routines, freeRTOS was employed in this project. FreeRTOS is an open-source real-time operating system, designed for embedded systems with limited processing and memory resources. With features like task management, synchronization, and inter-task communication, freeRTOS enables efficient coordination in multi-tasking environments [26].

Since the code is quite extensive, it is important to understand its operation through the following block diagrams. These diagrams offer a visual representation of the code structure and flow, aiding in comprehension.

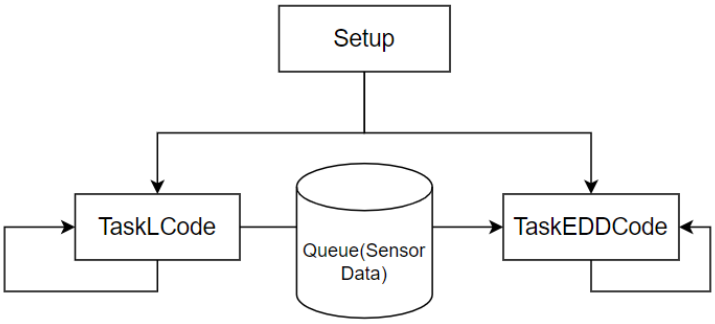

Fig. 4. Code flow block diagram for the input microcontroller.

Figure 4 illustrates the code flow on the input microcontroller. In the Setup block, the initialization of communications protocol takes place. In the Setup block, tasks are also initialized and defined, specifying their priority, stack memory, and core utilization. TaskLCode is responsible for continuously reading sensor parameters and sending all relevant data to TaskEDDCode. TaskEDDCode is responsible for receiving all the data and forwarding all sensor parameters to the Rpi.

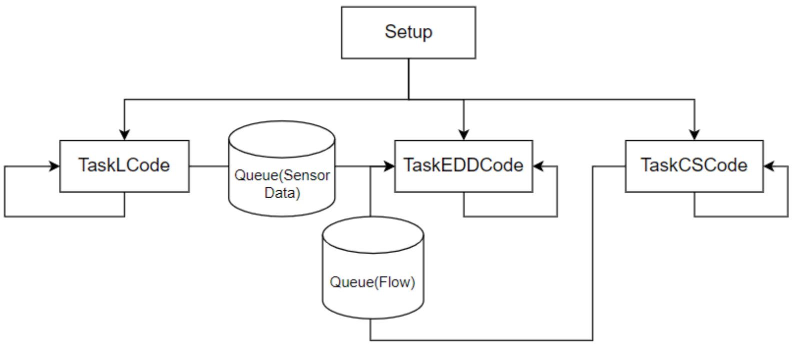

Fig. 5. Code flow block diagram for the output microcontroller.

The firmware present in the output microcontroller contains the same code as the one in the input microcontroller, with the addition of just one extra task. This task is responsible for flow measurement (calculating the time and relating it to the volume of the container) in the output measuring container, as well as sending the command signal to activate the output drain pump. Figure 5 illustrates the functional diagram of the code implemented in the output microcontroller.

It is important to note that all the tasks in both microcontrollers operate within an infinite loop and are independent of each other. To ensure that sensor data and flow measurements is not accessed simultaneously by both tasks, data synchronization methods such as queues are employed. This ensures that the shared resource (sensor data and flow measurements) maintains its data integrity and prevents unexpected or erroneous behaviors. These methods enhance the robustness of the routine and the viability of the gathered data [26].

2.6. Higher levels routines

In this work, two ESP32 microcontrollers are responsible for collecting sensor data, which is then transmitted to the Rpi using the MQTT protocol. The Rpi acts as a broker, facilitated by the Mosquitto application, allowing it to receive messages published by the ESP32 devices. These messages contain the sensor data and are organized into topics. The broker ensures that the data from the ESP32 microcontrollers is reliably and efficiently delivered to the Rpi.

In addition to its role as a broker, the Rpi plays a crucial role in retrieving data from the CleanGrow200 module using the HTTP protocol. Through the HTTP protocol's functions of PUT and GET, the Rpi establishes a communication channel with the CleanGrow200 module, allowing it to send requests for data and retrieve the corresponding responses.

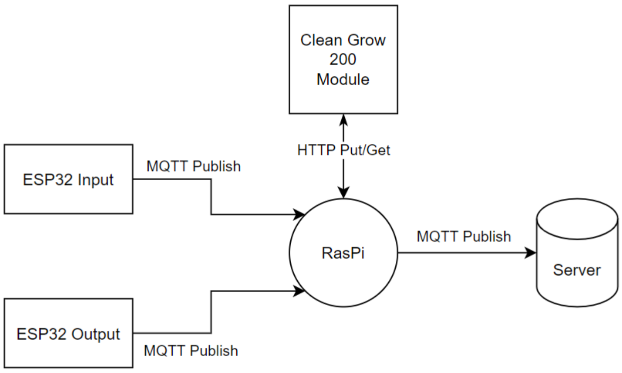

Fig. 6. Raspberry Pi, ESP32, CleanGrow200, and Server diagram.

With the combination of MQTT and HTTP protocols, the Raspberry Pi (as shown in Figure 6) acts as a central hub, receiving sensor data from the ESP32 devices via MQTT and retrieving data from the CleanGrow200 module using HTTP's PUT and GET functions. To facilitate this communication, a Python script was developed to handle the data exchange between the devices. The script establishes MQTT subscriptions to receive sensor data and utilizes HTTP requests to interact with the CleanGrow200 module. By seamlessly integrating these protocols, the system ensures efficient data transfer and synchronization between the different components, enabling real-time monitoring and analysis of water parameters.

This seamless integration of communication protocols enables efficient data transfer and empowers the system to make informed decisions based on real-time sensor readings and control commands.

2.7. MRIPTA

In order to store and present data in real-time, a specialized framework hosted on the Polytechnic Institute of Tomar (IPT) server called "MRIPTA" (*Monitorização Remota de Infraestrutura Piloto de Tratamento de Águas residuais por via biológica,* which can be translated as "Remote monitoring of a biological pilot-scale wastewater treatment plant") was employed. This framework is specifically designed for monitoring and managing pilot infrastructure for biological wastewater treatment. MRIPTA provides a comprehensive set of tools and functionalities to collect, store, and visualize data from various sensors and actuators in the wastewater treatment system.

The MRIPTA framework utilizes the MQTT protocol to receive and store data in real-time. It provides a comprehensive platform for data analysis, allowing users to visualize the collected data through intuitive bar and line graphs. Additionally, the framework offers the flexibility to export stored data to Excel for further in-depth analysis and reporting.

3. MATERIALS AND METHODS

3.1. Pilot-scale CW

Two small pilot-scale CW were the basis of the data acquisition framework described in this work. A square-shaped modular CW with 1.19 m^2 of surface area, filled with a mixture of limestone waste, cork waste, and coal slag, and a rectangular modular CW with 2.39 m^2 of surface area, filled with a mixture of limestone waste and fragmented clay bricks. Both CW are of subsurface flow type and are planted with common reeds (*Phragmites australis*).

The square-shaped CW is fully described elsewhere [16]. The rectangular CW has been developed under the EcoModZHC project (http://www.ecomodzhc.ipt.pt/en/).

3.2. Sensors and actuators

EC and pH sensors were purchased from AtlasScientific (US), model EZO-EC and EZO-pH, respectively. EC and pH sensors have in-built temperature probes.

NTU SN-PNEP turbidity sensors were acquired from Aqualabo Ponsel (FR).

ZATA (HK) ZWQ-COD sensors were applied to estimate the content of organic matter in the CW's water streams. This kind of sensor is based on the absorbance of 254 nm UV radiation by organic molecules in the water.

In addition to the parameters mentioned above, the concentration of phosphates, and nitrates, among other ions, was determined through an integrated sensor system from Clean Grow (UK), model CG200.

A compact weather station (ZATA, HK, model ZWS) provides useful data, such as wind speed, air temperature, humidity, rainfall, and solar radiation. The information provided by the weather station helps to determine the relevance of the measured parameters to the water treatment process.

Capacitive level sensors SEN0204 from DFRobot (CN) were utilized to measure the water level in the output measuring container. These sensors do not require direct contact with the liquid.

A peristaltic pump BT100S from LeadFluid (PRC), was used at the system's inlet. This ensures that the residues present in the wastewater do not affect the pump's functionality and allows for precise and accurate flow control. This peristaltic pump was selected because it can be powered by DC voltage and enables read-and-write data communication through a protocol explained next.

A JT-180 submersible pump (DFRobot, CN) was used for pumping the treated water into the water storage tanks.

3.3. Grid-independent energy system

In order to make the system self-sustainable, the decision was made to utilize photovoltaic (PV) solar modules. This renewable energy source is abundant in the geographical area where the PV modules will be installed, and additionally, the prices of solar equipment have been decreasing.

To design the PV system, a simple energy assessment was carried out. The expected power consumption was computed by adding the individual power consumption from the installed hardware in the system, using equation (1).

$$P_{total} = \sum_{i=1}^{N} n_i P_i \tag{1}$$

where n_i is the number of units of each piece of equipment, and P_i is the power consumption of each piece of equipment.

Knowing the total power required by the system, the calculation of the energy required during a day (E_a) can be carried out using Eq. (2), were h is the efficiency of the energy conversion and storage system.

$$E_a = 24P_{total}/\eta \tag{2}$$

With the calculated daily energy required, the peak power calculation of the photovoltaic panels, P_{peak}, can be carried out using Eq. (3), were N_h is the equivalent number of hours of peak radiation per day (1kW/m^2) in the system location. It should be used the month in which this value is lower (worst situation). There are several databases available online that, by inputting the location of the system, allow to attain the peak sun hours in a particular month.

$$P_{peak} = E_a/N_h \tag{3}$$

Equation (4) allows to calculate the number of PV panels, *Ns*, to be put in series, to attain the necessary voltage, based on the battery voltage, B_v, and the panel voltage, P_v.

$$N_S = \frac{B_V}{P_V} \qquad (4)$$

Equation (5) uses the peak power needed, P_{peak}, and also N_s and P_p (the PV power of each panel), to attain the number of string panels to put in parallel.

$$N_P = \frac{P_{peak}}{N_S\, P_P} \qquad (5)$$

These calculations ensure the proper configuration of the photovoltaic system to meet the voltage and power requirements effectively.

To calculate the number of batteries to be paralleled, (B_p), that are required to ensure energy independence, equation´s (6) and (7) would be used [27].

The amount of charge, C_M, assuming a five-day autonomy period, considering a recommended deep of discharge, D_R, can be calculated using Equation (6).

$$C_M = 5\,\frac{E_a}{0.8B_V} \qquad (6)$$

The anterior calculation is used as an input in equation (7) to determine the necessary battery capacity to sustain the system's energy requirements during periods of low sunlight or unfavorable conditions. Knowing the required amount of charge, and assuming a battery capacity, B_C, (in Ah), the number of batteries connected in parallel (B_P) necessary to power the entire system can be calculated using Eq. 7.

$$B_P = \frac{C_M}{B_C} \qquad (7)$$

It is important to note that a charger with MPPT (Maximum Power Point Tracking) algorithm should be placed downstream of the panels and upstream of the batteries to ensure optimal charging by utilizing the maximum available power [28].

4. RESULTS AND DISCUSSION

4.1. Examples of the data acquired by the sensor network

With the implementation of the comprehensive monitoring system, including the MRIPTA framework, the wastewater treatment process has undergone a significant transformation. This integrated system not only utilizes advanced technologies such as MQTT and real-time data acquisition but also incorporates sophisticated analysis and visualization capabilities. By capturing and processing data from various sensors and devices, the monitoring system provides a comprehensive overview of the wastewater treatment process.

The graphs generated by the MRIPTA framework provide a comprehensive visualization of several important parameters in the wastewater treatment process. These graphs offer valuable insights into the performance and efficiency of the system. By analyzing these graphs, researchers can identify trends, anomalies, and correlations among different parameters, facilitating informed decision-making and timely adjustments to optimize the wastewater treatment process.

Figures 7 to 9 provide a snapshot of one day's worth of data captured and displayed on the MRIPTA platform. Figure 7 presents the air humidity levels, offering insights into the atmospheric moisture content throughout the day. Figure 8 showcases two plots, one depicting the variations in air temperature and the other displaying the changes in water temperature over time. These temperature profiles are essential for assessing the influence of temperature on chemical parameters within the CW system. Finally, Figure 9 focuses on the pH levels at the system's input and output points, providing a comparison of the acidity or alkalinity of the incoming and treated water.

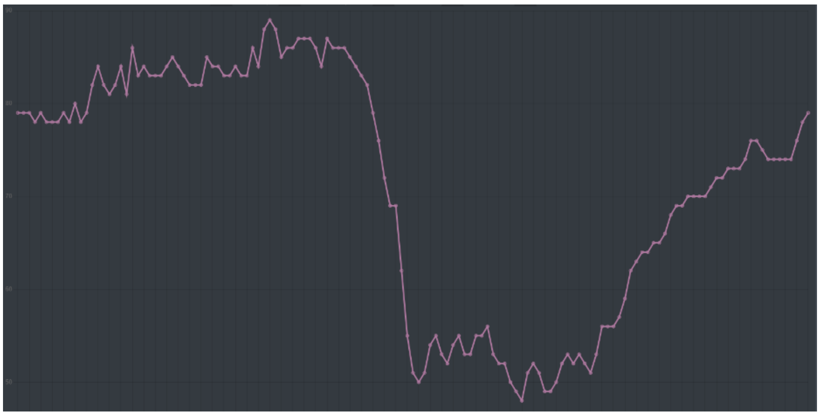

Fig. 7. Typical daily air humidity variation.

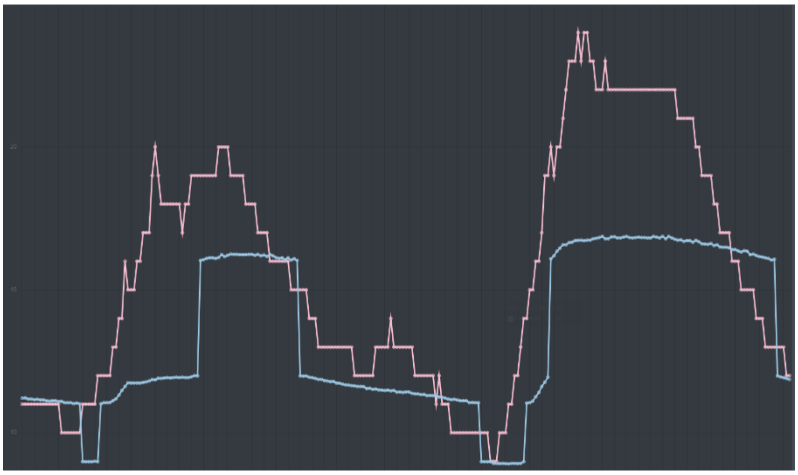

Fig. 8. Typical daily water (blue) and air (pink) temperature variation.

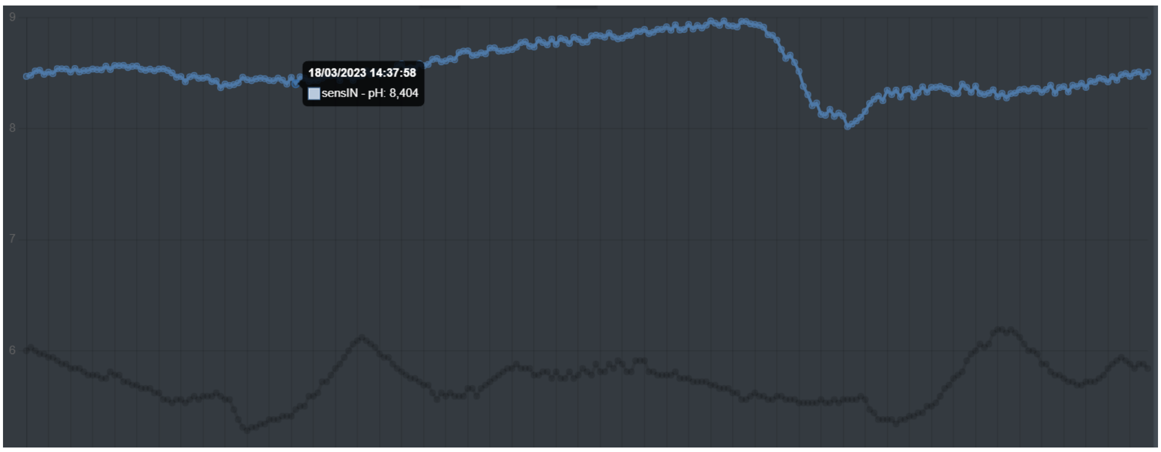

Fig. 9. Typical daily pH variation: input of wastewater (light blue); output of treated water (dark blue).

The combination of the DCS with the MRIPTA platform provides a comprehensive visualization of the important parameters discussed earlier, allowing for a simultaneous comparison, and plotting of multiple variables. These interactive graphs offer a detailed visualization of crucial parameters such as air humidity, air and water temperature, and pH levels. This comprehensive view enables researchers to monitor and analyze the performance of the wastewater treatment system in real time. In addition to the real-time visualization provided by the MRIPTA platform, it also offers the functionality to export the data to Excel for further analysis and comparison. This feature enables users to delve deeper into the collected data, perform advanced calculations, and conduct comprehensive evaluations.

4.2. Implemented Energy system

To design the PV system, a simple energy assessment was carried out. The expected power consumption was computed by adding the individual power consumption from the installed hardware in the system.

Table 2 displays the operating voltages and current consumption of all the main sensors and actuators in the CW system. By summing up these values, a total power required by the system of 85.133 W was determined by using Eq. (1).

Since the system ideally should be independent of the electrical grid, all calculations should be performed for the worst possible cases of irradiance.

Knowing the total power, the calculation of the energy required during a day (E_a) can be carried out using Eq. (2).

Equipment	Quantity	Current draw per unit	Total current draw	Rated voltage	Mean power required
Level sensor	2	0.01 A	0.02 A	5 V	0.1 W
ESP 32	2	0.3 A	0.6 A	5 V	3 W
Raspberry Pi	1	2 A	2 A	5 V	10 W
Clean Grow 200	2	0.5 A	1 A	5 V	5 W
Peristaltic pump	1	1.6 A	1.6 A	36 V	60 W
Drain pump	1	0.2 A	0.2 A	5 V	1 W
pH sensor	2	0.001 A	0.002 A	3.3 V	6.6 mW
EC sensor	2	0.001 A	0.002 A	3.3 V	6.6 mW
Turbidity sensor	2	0.0015 A	0.003 A	12 V	36 mW
Organic matter sensor	2	0.001 A	0.002 A	12 V	24 mW
Weather station	1	0.08 A	0.08 A	12 V	0.96 W
Auxiliary electronics	-	-	1 A	5 V	5 W

Table 2. Power consumption of individual components

To allow some flexibility in the PV system component selection, it is considered a “relatively poor efficiency” of the energy conversion and storage system (h = 60%). Like this, the energy required during a day is 3405 Wh.

With the calculated daily energy required, the peak power calculation of the photovoltaic panels can be carried out using Eq. 3. With N_h being the equivalent number of hours of peak radiation per day, in the month in which its value is lower.

There are several databases available online. Using data from the National Renewable Energy Laboratory (NREL) [29] by inputting the location of the system; a tilt of 35º and an azimuth of 180º, a value of 2.71 peak sun hours is obtained (in December). This is the month considered, as it has the lowest number of hours of maximum solar radiation compared to the other months of the year.

From this value, using Eq. (3), a peak power, P_{peak}, of 1147 Wp was estimated for the set of photovoltaic panels.

A survey was conducted to assess photovoltaic panels, batteries, and regulators for the system. The key selection parameters for the panels were power and peak voltage. The battery selection criteria included energy storage capacity and output voltage. The regulator was chosen based on its nominal power, charging voltage, and charging algorithm. It is important to note that factors such as price and component delivery speed also played a significant role in the selection process. After careful analysis and consideration, the DMEGC "DM550M10-72HSW/-V", 550 W photovoltaic panels, Kaise "KBAS122500" batteries, and Victron "SmartSolar MPPT 150/45" MPPT regulator were chosen. Victron "Orion-Tr 48/12-20" converter is also used to attain 12V for the electronics.

Knowing the peak power (P_P = 550 Wp) and the peak voltage of each panel (P_V = 41 V), and the charging voltage of the batteries (B_V = 48 V), the number of panels in series (N_S, Eq. (4)) and the number of panels in parallel (N_P, Eq. (5)) required to achieve the desired voltage and power, respectively, were calculated. After rounding, the achieved N_s is 2, giving N_p = 1.0427, this value has been rounded to 2, which leaves a big safety margin. These calculations ensure the proper configuration of the photovoltaic system to meet the voltage and power requirements effectively.

To calculate the number of systems of batteries to be paralleled, (B_p), that are required to ensure energy independence, the amount of charge (C_M) for a five-day autonomy period, considering a deep of discharge, D_R, of 0.8 was first calculated using Equation (6) [27]. The battery capacity requirement, estimated from Eq. (6), is 443 Ah.

Knowing the required amount of charge, the number of batteries connected in parallel (B_P) necessary to power the entire system can be calculated using Eq. (7). The value of the battery capacity, $B_{C,}$ stated in the technical datasheet was used for this calculation (B_C = 250 Ah), conducting to a number of required batteries in parallel of 1.773, rounded off to 2.

It can be concluded that to ensure energy supply to the entire system for a period of five days under the worst irradiance conditions, with the identified material chosen, two paralleled sets of two photovoltaic panels connected in series, and two strings of 48V battery systems in parallel (eight 12V batteries) are required, as represented at Figure 10.

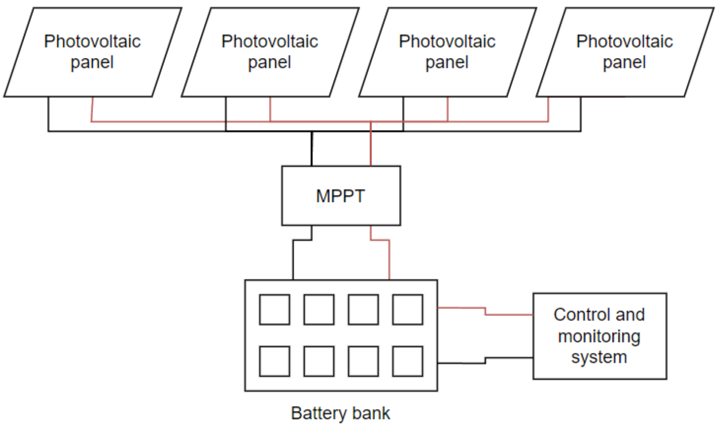

Fig. 10. Connection diagram of the off-grid photovoltaic system.

5. CONCLUSIONS

Constructed Wetlands, as well as other Nature-Based Solutions, are a sustainable, cost-effective, and eco-friendly technology for wastewater treatment and recovery. However, CW monitoring and control is difficult because its efficiency depends on several interconnected mechanisms, all of which are affected by environmental variables.

The development of effective data acquisition based on sensors and IoT devices can contribute to a better understanding of the mechanisms underlying the effectiveness of wastewater treatment by CW.

The monitoring system described in this work demonstrates, after its effective start-up, that a set of useful data can be obtained. As expected, it was observed that most water quality parameters showed a significant daily variation. Considering that the common monitoring of CW relies on low-frequency water sampling, knowing the accurate trend from high-frequency data acquisition through the sensor network can allow further improvement of CW operation.

In addition to the sensor network design, the project of an energy system based on photovoltaic panels and batteries showed that the affordable energy autonomy of CW systems can be achieved. This result can be applied to the design of decentralized CW facilities, namely to provide wastewater treatment and reuse in low-density villages and remote agroindustrial sites.

Further work will focus on the application of data science tools to the gathered data, which goal is the conception of control models to allow the development of a smart framework that allows self-adaptation of CW operation to the wastewater characteristics and weather variables.

ACKNOWLEDGMENTS

This research was supported by the Smart Cities Research Center under the grants UIDB/05567/2020 and UIDP/05567/2020 funded by The Portuguese Foundation for Science and Technology (FCT – Fundação para a Ciência e a Tecnologia, Portugal). The grant CENTRO-01-0145-FEDER-179932 (EcoModZHC project) is also acknowledged. The authors also thank the support of the BIOTEC.IPT Lab, Ci2, Lab.IPT and all supporting services of Politécnico Instituto de Tomar.

REFERENCES

1. The Council of the European Communities 1991, *Urban Waste Water Treatment Directive (91/271/EEC) of 21 May 1991*, viewed 23 July 2023, <https://www.era-comm.eu/EU_water_law/stand_alone/part_4/index.html>

2. Tchobanoglous, G, Stensel, H, Tsuchihashi, R, Burton, F 2013, "Wastewater Engineering: Treatment and Resource Recovery", McGraw-Hill Education, New York.

3. European Commission Water Directors: Amsterdam, The Netherlands, 2016, *EC. Guidelines on Integrating Water Reuse into Water Planning and Management in the Context of the WFD*, viewed 27 July 2023, <https://ec.europa.eu/environment/water/pdf/Guidelines_on_water_reuse.pdf>

4. Rebelo, A, Quadrado, M, Franco, A, Lacasta, N, Machado, P 2020, "Water reuse in Portugal: New legislation trends to support the definition of water quality standards based on risk characterization", Water Cycle, vol. 1, pp. 41–53. https://doi.org/10.1016/j.watcyc.2020.05.006

5. Neczaj, E, Grosser, A 2018, "Circular Economy in Wastewater Treatment Plant–Challenges and Barriers", *Proceedings*, 2(11), 614. https://doi.org/10.3390/proceedings2110614

6. Hagenvoort, J, Ortega-Reig, M, Botella, S, García, C, de Luis, Ac, Palau-Salvador, G 2019, "Reusing Treated Waste-Water from a Circular Economy Perspective-The Case of the Real Acequia de Moncada in Valencia (Spain)", *Water*, 11(9), 1830. https://doi.org/10.3390/w11091830

7. Furumai, H 2008, “Rainwater and reclaimed wastewater for sustainable urban water use”, Physics and Chemistry of the Earth, Parts A/B/C, vol. 33, pp. 340–346. https://doi.org/10.1016/j.pce.2008.02.029
8. Digiano, FA, Weaver, CC, Okun Deceased, DA 2009, “Benefits of shifting fire protection to reclaimed water”, J. Am. Water Works Assoc., vol. 101, pp. 65–74. https://doi.org/10.1002/j.1551-8833.2009.tb09840.x
9. Cherchi, C, Kesaano, M, Badruzzaman, M, Schwab, K, Jacangelo, JG 2019, “Municipal reclaimed water for multi-purpose applications in the power sector: A review”, J. Environ. Management, vol. 236, 561–570. https://doi.org/10.1016/j.jenvman.2018.10.102.
10. Pinho, HJO, Mateus DMR 2021, “Sustainable production of reclaimed water by constructed wetlands for combined irrigation and microalgae cultivation applications”, Hydrology, vol. 8, no. 1:30. https://doi.org/10.3390/hydrology8010030
11. Pinho, HJO, Mateus DMR 2022, “Contribution of Constructed Wetlands for Reclaimed Water Production: A Review”, IOP Conf. Ser.: Earth Environ. Sci., vol. 1006 012008. https://www.doi.org/10.1088/1755-1315/1006/1/012008
12. Ren, X, Zhang, Y, Chen, H 2020, “Graywater treatment technologies and reuse of reclaimed water for toilet flushing”, Environ. Sci. Pollut. Res., vol. 27, pp. 34653–34663. https://doi.org/10.1007/s11356-019-05154-6
13. Frantzeskaki, N 2019, “Seven lessons for planning nature-based solutions in cities”, Environ. Sci. Policy, vol. 93, pp. 101–111. https://doi.org/10.1007/s11356-019-05154-6
14. Pearlmutter, D, Theochari, D, Nehls, T, Pinho, P, Piro, P, Korolova, A, Papaefthimiou, S, Mateo, M.-CG, Calheiros, C, Zluwa, I, Pitha, U, Schosseler, P, Florentin, Y, Ouannou, S, Gal, E, Aicher, A, Arnold, K, Igondova´, E, Pucher, B 2020. “Enhancing the circular economy with nature-based solutions in the built urban environment: green building materials, systems and sites”, Blue Green Syst., vol. 2 (1), pp. 46–72. https://doi.org/10.2166/bgs.2019.928
15. Mateus, DMR, Pinho, HJO 2018, “Screening of Solid Waste as Filler Material for Constructed Wetlands”, *IOP Conf. Ser. Earth Environ. Sci.*, 182, 012001. https://doi.org/10.1088/1755-1315/182/1/012001
16. Pinho, HJO, Mateus DMR 2022b “Chapter 13 – Valorization of solid waste in subsurface flow constructed wetlands based on renewable modular structures: A contribution to a circular economy”, in: Stefanakis, A, Nikolaou, I (eds), *Circular Economy and Sustainability*, Elsevier, pp. 215-233. https://doi.org/10.1016/B978-0-12-821664-4.00019-4
17. Kadlec, RH and Wallace, S 2009, “Treatment Wetlands”, 2nd Edition, Taylor & Francis, Boca Raton. https://doi.org/10.1201/9781420012514
18. Mateus DMR, Pinho, HJO 2020, “Evaluation of solid waste stratified mixtures as constructed wetland fillers under different operation modes”, *Journal of Cleaner Production*, vol. 253, 119986, https://doi.org/10.1016/j.jclepro.2020.119986
19. Pinho, H. et al. 2023, “Smart Monitoring of Constructed Wetlands to Improve Efficiency and Water Quality”, in: Xu, H (eds), *Proceedings of the 5th International Symposium on Water Resource and Environmental Management*. WREM 2022. Environmental Science and Engineering. Springer, Cham. https://doi.org/10.1007/978-3-031-31289-2_15
20. NXP 2021, “*I2C-bus specification and user manual*”, viewed 27 July 2023, <https://www.nxp.com/docs/en/user-guide/UM10204.pdf>
21. Modicon 1996, “*Modbus Protocol Reference Guide*”, <https://www.modbus.org/docs/PI_MBUS_300.pdf>
22. Microship 2017 ,”*UART reference manual*”, viewed 27 July 2023, <https://www.microchip.com/DS60001107>

23. Standford-Clark and Truong, 2013, "*MQTT For Sensor Network*" (MQTT-SN), viewed 27 July 2023, <https://www.oasis-open.org/committees/download.php/66091/MQTT-SN_spec_v1.2.pdf>
24. OASIS 2019, "*MQTT Version 5.0*", viewed 27 July 2023, <https://docs.oasis-open.org/mqtt/mqtt/v5.0/mqtt-v5.0.html>
25. The Internet Society 1999, "*Hypertext Transfer Protocol – HTTP/1.1*", viewed 27 July 2023, <https://datatracker.ietf.org/doc/html/rfc2616#section-9.3>
26. FreeRTOS and Richard Barry 2016, "*Masterial the FreeRTOS Real Time Kernel*", viewed 27 July 2023,<https://www.freertos.org/fr-content-src/uploads/2018/07/FreeRTOS_Reference_Manual_V10.0.0.pdf >
27. M. Alramlawi, Y. Souidi and P. Li, 2019. "Optimal design of PV-Battery Microgrid Incorporating Lead-acid Battery Aging Model," IEEE International Conference on Environment and Electrical Engineering and 2019 IEEE Industrial and Commercial Power Systems Europe (EEEIC / I&CPS Europe), Genova, Italy, 2019, pp. 1-6. https://doi.org/10.1109/EEEIC.2019.8783927
28. D. Benedetti, J. Agnelli, A. Gagliardi, P. Dini and S. Saponara, "Design of an Off-Grid Photovoltaic Carport for a Full Electric Vehicle Recharging," 2020 IEEE International Conference on Environment and Electrical Engineering and 2020 IEEE Industrial and Commercial Power Systems Europe (EEEIC / I&CPS Europe), Madrid, Spain, 2020, pp. 1-6. https://doi.org/10.1109/EEEIC/ICPSEurope49358.2020.9160655
29. National Renewable Energy Laboratory, *"PVWatts® Calculator, Solar Resource Data, NREL, U.S. Department of Energy, Website Version 8.2.1"*, viewed 27 July 2023, <https://pvwatts.nrel.gov/pvwatts.php>.